I. M. Templeton, J. Phys. E 4, 414 (1971).
[23]A. B. Pippard, *The Dynamics of Conduction Electrons* (Gordon and Breach, New York, 1965), p. 21.
[24]G. B. Scott, M. Springford, and J. R. Stockton, J. Phys. E 1, 925 (1968).
[25]J. Vanderkooy and W. R. Datars, Phys. Rev. 156, 671 (1967).
[26]Model 1411, Weston Instruments Division, Newark, N. J. 07114.
[27]A. Goldstein, S. J. Williamson, and S. Foner, Rev. Sci. Instr. 36, 1356 (1965).
[28]R. W. Stark and L. R. Windmiller, Cryogenics 8, 272 (1968).
[29]Model 2T60-1110 with a modified S-10 speed controller, G. H. Heller, Las Vegas, Nev. 89114.
[30]R. G. Poulsen, J. S. Moss, and W. R. Datars, Phys. Rev. B 3, 3107 (1971).
[31]A. C. Thorsen and T. G. Berlincourt, Rev. Sci. Instr. 34, 435 (1963).
[32]Molykote Z, Dow Corning Corp., Midland, Mich. 48640.
[33]E. R. Andrew, I. Roberts, and R. C. Gupta, J. Sci. Instr. 43, 936 (1966).
[34]Adhesive and insulating varnish No. 7031, General Electric, Schenectady, N. Y. 12305.
[35]Type FA-135-173, Wallace & Tiernan, 25 Main St., Belleville, N. J. 07109.
[36]B. R. Watts, Proc. Roy. Soc. (London) A282, 521 (1964).
[37]J. B. Ketterson and L. R. Windmiller, Phys. Rev. B 2, 4813 (1970).
[38]L. R. Windmiller, J. B. Ketterson, and S. Hörnfeldt, Phys. Rev. B 3, 4213 (1971).
[39]J. B. Ketterson, L. R. Windmiller, and S. Hörnfeldt, Phys. Letters 26A, 115 (1968).
[40]J. S. Lass and A. B. Pippard, J. Phys. E 3, 137 (1970).
[41]P. B. Visscher and L. M. Falicov, Phys. Rev. B 2, 1518 (1970).

PHYSICAL REVIEW B VOLUME 6, NUMBER 4 15 AUGUST 1972

Electronic Structure of Noble-Metal–Noble-Metal Alloys†

David Beaglehole*
Physics Department, University of Maryland, College Park, Maryland 20742

and

Erich Erlbach‡
City College of the City University of New York, Convent Ave., New York 10031

(Received 3 December 1971)

We describe optical studies of dilute noble-metal–noble-metal alloys. A differential technique compared the reflectance of the alloy with the reflectance of the pure metal and measured a quantity proportional to just the difference in reflectance. The method was particularly sensitive to small changes in reflectances and could be used to study very dilute alloys—the alloys here were between $\frac{1}{10}$- and 3-at.% impurity concentration. The measurements indicated that the noble alloys are of two types. In copper-gold and silver-gold alloys the electron energy bands shift smoothly as the concentration varies. The rates and directions of shifts are determined not only by differences in the host and impurity potentials, but also by the changes in lattice constant, and we emphasize the importance of the latter. In contrast, in copper-silver alloys separate host and impurity *d* bands are formed.

I. INTRODUCTION

While the electronic structure of metal crystals is now fairly well understood, the theory of alloys is still rudimentary. The difficulty is that common to all disordered systems (liquid, amorphous, and alloys)—the difficulty of including the correlation effects involved in a random distribution of atoms. In two limits, however, the theory is well based.[1] In the weak-perturbation limit, when the components disturb each other only slightly when mixed, the energy levels should move smoothly from those characteristic of one component to those characteristic of the other as the concentration varies. In the strong-perturbation limit, when the energies and wave functions of the two components are very different, the electrons should maintain their individual character and form localized or resonant states. Recently, the coherent-potential theory[2–4] has provided a link between these two extreme limits, though the theory at present is based on rather simple assumptions concerning the interaction of electrons on different sites.

Experimentally it is of interest to study how various alloy systems fit into the range of perturbation behaviors. Optical experiments are particularly useful, since they measure the excitation of electrons between allowed energy levels and can distinguish between the weak- or strong-perturbation situations and measure changes in energy levels.

In this paper we describe an optical study of the noble-metal–noble-metal series of alloys (we will call these the noble alloys). The noble alloys have various unusual properties. Silver and gold have almost exactly the same lattice spacing, mixing with little change in lattice constant. Copper has a smaller lattice spacing and contracts the silver or gold lattice on alloying.[5] In gold-silver alloys then, changes in electronic structures will be due only to differences in atomic potential, while in copper-gold and copper-silver alloys, changes in lattice constant will also affect the energy levels. The noble-alloy phase diagrams are also unusual.[6] Gold and silver, and gold and copper, are miscible in all proportions, while copper and silver are only miscible up to concentrations of a few percent.

Optical studies of the noble metals have shown that the main absorption edge, occurring in the red, yellow, and ultraviolet for copper, gold, and silver, respectively, is associated with excitation of d electrons to states above the Fermi level. Absorption edges at higher energies are associated with excitation of both conduction electrons and d electrons. For example, Segall's band structure[7] for copper is shown in Fig. 1. That for silver is similar, with the d band lying around the bottom of the conduction band. The general behavior for gold is also similar, but here degeneracies are split by a sizable spin-orbit interaction, and the topmost d-band level occurs near X rather than L. The main absorption edges in these metals occur from transitions from the upper d level to the Fermi surface, while the conduction-electron transitions are around the neck L_2' to L_1 (and its equivalent in gold). Values for the main energy gaps are listed in Table I.

Of the noble alloys only the gold-silver system has been studied previously, and measurements by Wessel,[8] Fukutani and Sueoka,[9] and Rivory[10] have shown a smooth shift of the main absorption edge from silver to gold, i.e., weak-perturbation behavior. Faraday-effect measurements by McAlister *et al.*[11] and de Haas–van Alphen measurements[12] by Chollet and Templeton and King-Smith have shown smooth shifts in Fermi-surface topology.

We have used a differential reflectance technique[13] to measure the change in reflectance of the pure metal on addition of small amounts of other noble metals, for all six dilute noble alloys. The technique was developed previously for studies of dilute Au-Fe alloys.[14] The reflectance of a pure sample R_p was compared with that of a dilute alloy R_a, and the quantity related to the difference in reflectivity $(R_p - R_a)/(R_p + R_a)$ was recorded continuously as a function of wavelength.

The method is particularly suited to dilute alloy studies, since systematic errors are removed by the comparison technique, and, further, the method is sensitive to the effects of small amounts of impurity since zero signal is recorded when the reflectance is unchanged. The high sensitivity in fact

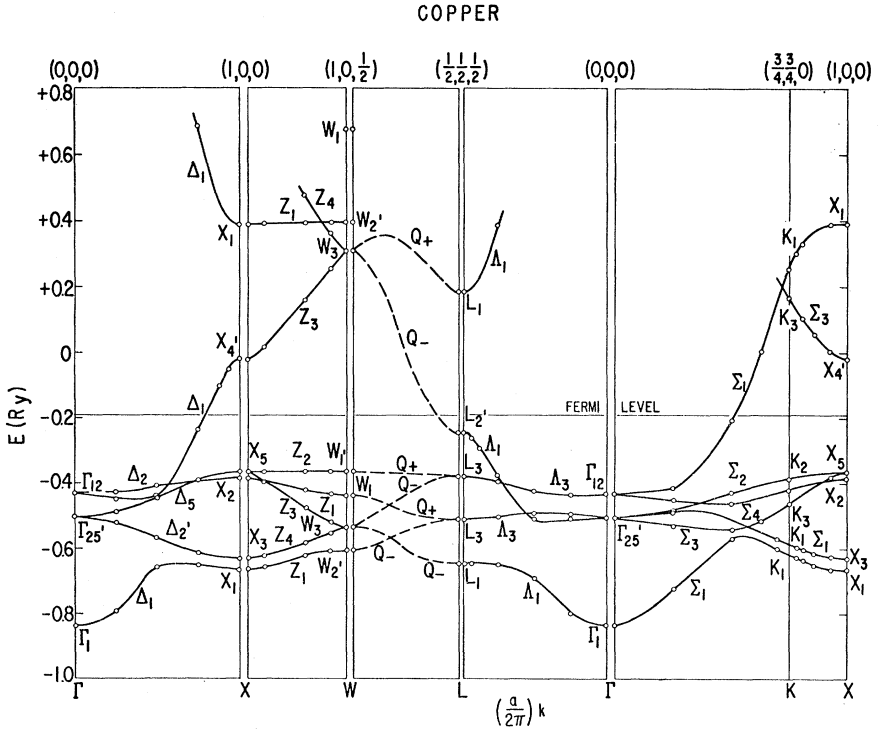

FIG. 1. Band structure of copper, as calculated by Segall, Ref. 7.

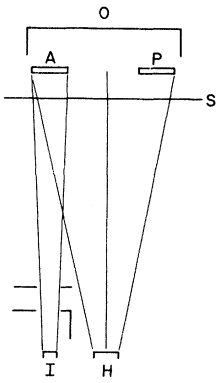

FIG. 2. Evaporation system. H and I are the host and impurity boats, respectively, P and A the pure and alloy substrates, and O the oven.

has allowed us to make studies at concentrations sufficiently low that the impurity atoms should be only weakly interacting with each other, and at concentrations sufficiently low that lifetime broadening due to the presence of the impurity was less than induced energy shifts. We have been able to study the copper-silver system with samples annealed in its stable-solution range.

An outline of the results has been published in Ref. 15, and comments on the gold alloys in Ref. 16. Here we give a comprehensive account of this study.

II. SAMPLE PREPARATION

For this study samples were needed with smooth clean surfaces. Bulk samples usually have scratch marks and uneven surfaces which would cause reflectance variations much larger than those induced by dilute alloying. Rather, we have used films evaporated onto smooth substrates. Other workers have prepared alloy films either by evaporation from an alloy ingot,[10] or by alternate flash evaporation of pure and host pellets with subsequent heating to diffuse the layers.[11] A disadvantage of the first method is that the ratio of the components in the vapor is often very different from the ratio of the components in the ingot, and it is difficult to vary the film's concentration. A disadvantage of the second method is the following: We have found that no matter what cleaning precautions we have taken, when we melt a material a scum is always present, which takes a little time to evaporate away. In the flash-evaporation technique the scum material must fall also onto the substrate, adding an uncertain impurity to the alloy.

We have used a technique of simultaneous evaporation of host and impurity from separate boats. With this method the vapor pressure of the two components could be varied independently and a shutter left closed until all scum material had disappeared. A further consideration determined our evaporation geometry. In practice, we have found that two pure samples prepared by evaporation on different occasions differed in reflectance by up to 1%, but differed by much less, one or two tenths of a percent, if prepared at the same evaporation. Therefore, as in our earlier studies,[14] we have made our comparison pure samples and alloy samples simultaneously.

The technique was to mount two substrates in the evaporator (Fig. 2) and to use separate resistance-heated boats for host and impurity materials. The geometry was arranged so that the impurity vapor fell onto only one substrate, the host vapor symmetrically reaching both substrates. Thus when the boats were adjusted to appropriate temperatures and the shutter opened, an alloy was formed on the substrate seeing both boats, while a pure sample was prepared on the other substrate.

The concentration of the alloy depended upon the relative rates of evaporation from the two boats. We have tried to maintain these constant by evaporating away only fractions of the material in the boats. The samples were annealed immediately after preparation in the same vacuum system, and diffusion of the impurity across the thickness of the sample at the annealing temperature was sufficient to even out inhomogeneities due to the fluctuations in the evaporation rates.

Before evaporation the pressure in the chamber was less than 10^{-6} Torr, rising to about 2×10^{-6} Torr during evaporation. Evaporation rates were typically around 100 Å/sec for the host metal, the films being around 3000 Å thick.

The films were annealed immediately after preparation by moving a small heater to a position lying just above the two samples. The annealing conditions depended a little upon the alloy, but typically were about 500 °C for 10 min. The criterion we used was reproducibility of the optical measurement after a repeat anneal at the same condition. In our earlier studies of Au-Fe alloys we had found that high temperatures were essential, much more effective than lower temperatures for longer times. The shortest convenient time was 10 min, allowing for heating- and cooling-time constants. To find the optimum condition the temperature was raised until reproducible results were obtained. It was not possible to carry out a very high-temperature heat treatment since this so encouraged crystal growth and migration that the surfaces became rough and scattered light. We found that the surface migration depended upon the substrate material. Using fused-quartz substrates gold-rich films could be satisfactorily annealed at 600 °C without noticeable surface roughening, but copper and especially silver were found to roughen at temperatures as low as 250 °C. Cleaved-mica substrates were used

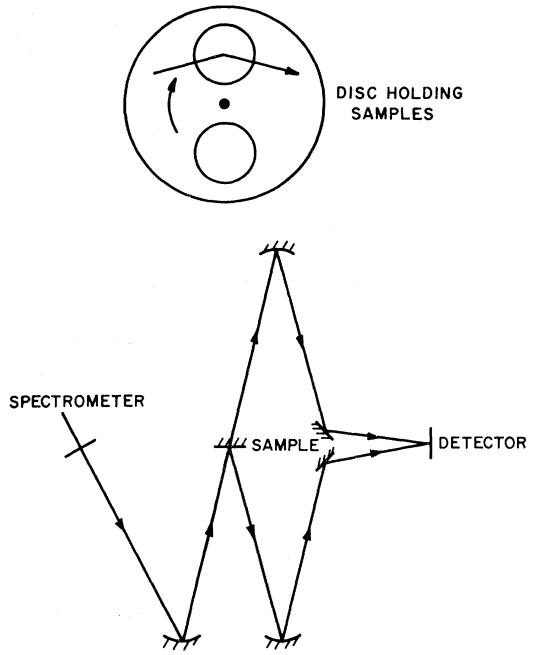

FIG. 3. Reflectometer optics. A rotating disk shown above holds the pure and alloy samples.

for the copper- and silver-rich alloys, the surfaces then remaining smooth up to temperatures greater than 500 °C.

As we mentioned in Sec. I, the gold-silver and gold-copper series were miscible in all proportions and there were no difficulties here arising from phase separation. The copper-silver system, however, had limited solubility. Hansen and Anderko[6] show the limits to be < 0.1 and 0.35 at. % at 200 °C for copper-silver and silver-copper, respectively, rising to 0.8 and 3 at. % at 500 °C, and to a maximum solubility of 5 and 15 at. %, respectively, near 800 °C. Thus care had to be taken to produce true alloy solutions. This was done by ensuring that the annealing temperatures lay within the equilibrium-solution range. Quick cooling of the samples then quenched-in the alloy solution. After the optical measurements we made careful x-ray studies of all the samples to check for signs of precipitation. We observed no new diffraction peaks at angles corresponding to those of the impurity, but only shifts in the angles of the host diffraction peaks as the lattice changed dimension. This showed that no phase separation had occurred.

Surface oxide layers were another potential source of difficulty in these sensitive measurements. Other studies[17] have shown that, fortunately, gold samples are stable in air, while oxide layers on copper are removed by heat treatment in an oil-diffusion pump vacuum (which has a residual reducing atmosphere). The copper samples were thus always cleaned by the annealing and reannealing process. However, we found that oxide layers on silver could not be removed by vacuum heating, and in this case all measurements and reannealing checks were made as quickly as possible after preparation, the process taking about 3 h to complete. Oxide effects became noticeable after delays of one-half a day.

It was difficult to obtain accurate concentrations in the dilute range since the customary x-ray-fluorescence and chemical-analysis methods are only sensitive to about 1 at. %. We have found approximate concentrations to about $\pm\frac{1}{3}$ at. % accuracy by measuring the resistance ratio of the alloys between room temperature and liquid-helium temperature. Values for the change of resistance of bulk metals on alloying were found many years ago by Linde.[18] At room temperature the resistance is determined by both phonons and impurities, at helium temperature only by the impurity. Thus, knowing the phonon and impurity resistivities, the ratio of the resistances at these two temperatures provided the concentration, independent of the sample's geometry. With films, however, there is a complication. The electron mean free path may become greater than the sample thickness at low temperatures, and the residual resistance depends then not only upon the impurity but also upon the electron scattering at the sample's surfaces. Dingle[19] has calculated corrections to find the equivalent bulk resistance in the limit of diffuse electron scattering at the surfaces. For specular scattering there is no correction.

The major uncertainty in finding the concentration by this method lay in knowing the degree of specularity of the electron scattering. The pure sample was useful here. The measured resistance ratio of pure sample on quartz was typically about 15, correcting to about 30 assuming diffuse electron scattering, quite a reasonable value for crystallites 1000 Å in diameter. The measured resistance ratios of pure samples on mica lay between 30 and 60, which would correct to values greater than 100 assuming diffuse scattering. In view of the values measured with quartz we have preferred to assume that mica substrates were so much smoother than quartz on an atomic scale that the electron scattering here was predominantly specular. The error of $\pm\frac{1}{3}$ at. % placed on the concentrations allows for the uncertainty in this assumption.

III. OPTICS

The pure and the alloy samples were mounted on a disk and spun on an axis inclined at a small angle to the light beam, as illustrated in Fig. 3. In this way the light beam was reflected first from the

pure sample and then from the alloy. If ω is the rotation frequency and R_p and R_a are the reflectivities of the pure and alloy samples, the ac signal at frequency ω was proportional to $(R_p - R_a)$, while the dc signal was proportional to $(R_p + R_a)$. The electronics was arranged to measure $(R_p - R_a)/(R_p + R_a)$, which we will denote by α. In measurements with small signals we have exchanged the pure and the alloy samples, repeated the measurement, and averaged the result, in order to avoid any systematic errors due to small misalignments of the disk. The light beam sampled the reflectivity of a strip across the samples. The resistance ratios were measured across the same strip.

If the alloy aperture was left open on the disk, the light would alternately be reflected and pass through. Mirrors were arranged so that this second beam was imaged also on the detector. In this case we measured $(1 - R_p)/(1 + R_p)$, from which the reflectivity of the pure metal could be evaluated. A full description of the optics may be found in Ref. 13.

In this study the measurements lay in the range 8000–1200 Å with a wavelength resolution of 10 Å. Between 2000 and 1200 Å we used a vacuum spectrometer, a hydrogen-discharge source, and a differential reflectometer set up in a vacuum chamber. The weaker light source led to more noise in this region, and stray light was more difficult to allow for. The results in this region have thus been used mainly to indicate reasonable extrapolations into the ultraviolet.

IV. REFLECTANCE MEASUREMENTS

First we present data illustrating various aspects of the experimental techniques. In Fig. 4(a) we show a test curve for α when no impurity was present. The two samples were both pure gold. Typically we found a small almost wavelength-independent signal, a "background" signal, positive or negative with different pairs, which was due to slight fractional differences in reflectance. Background values of α were less than 0.003 in the visible, increasing somewhat in the ultraviolet.

In Fig. 4(b) we illustrate the importance of annealing. One curve is for a 0.6-at.% unannealed copper-silver alloy, while the other curve shows the same alloy after annealing. The most important effect of annealing is to change a resonantlike (due to broadening) α at the main reflectance edge into a downwards peak. The curve was essentially unchanged after a second anneal.

In Fig. 4(c) we indicate the effect of too long a heat treatment. The pure sample which has higher surface mobility had become rough, and scattered a significant amount of light. A roughened surface decreases the reflectance[20] typically as $\Delta R \propto e^{-A/\lambda^2}$ and the α curve became superimposed upon a background which rose roughly parabolically. The sharp structure at all the reflectance edges is still to be seen.

In the following we now describe our results for annealed and smooth alloy samples. The alloys were made in the range $\frac{1}{10}$–3 at.%, 5 or so for each of the six dilute alloys. In Figs. 5–10 we show the measured α normalized to the change per unit atomic percent of impurity by dividing by the concentration—we plot α/c for the various samples.

We observe an interesting effect. In these figures it can be seen that only when the concentration was greater than about $\frac{1}{2}$ at.% did α become linear with concentration. Below this concentration the curves of α/c become greater the smaller the concentration, showing the nonlinear behavior. The nonlinearity is similar to the behavior observed earlier with Au-Fe alloys. We will discuss this later. Meanwhile we analyze the data in the linear region.

V. PURE-METAL DIELECTRIC CONSTANT

The response of solids to electromagnetic radiation is determined by their complex dielectric constant $\epsilon = \epsilon_1 + i\epsilon_2$. Here ϵ_1 measures the induced polarization and ϵ_2 the energy absorption. The spectra for the two components ϵ_1 and ϵ_2 for pure samples have been found from the reflectance data R_p by the well-known technique of Kramers-Kronig analysis. Our measurements lay in the region between 1.5 and 9 eV, while for the analysis it was necessary to have reflectance values over all energies. Below 1.5 eV we have used the infrared values of Bennett *et al.*[21] Beyond 9 eV we have taken R_p proportional to $(E)^{-C}$, where $E = \hbar\omega$ is the photon energy. The extrapolation parameter C was chosen so that calculated values of ϵ_2 in the visible agreed with reliable values in the literature. ϵ is made up of two contributions, part coming from excitations by conduction electrons within their band, the Drude intraband term, and part coming from excitations between bands, the interband term:

$$\epsilon = \epsilon_D + \epsilon_{1b} .$$

We will concentrate our attention for the most part on the imaginary part of the interband dielectric constant $\epsilon_{2\,1b}$, which at any energy is proportional to the sum of all interband transitions at that energy. Thus we have followed Ehrenreich and Philipp[22] in separating ϵ_2 into intra- and interband components. In the near infrared the frequency and conduction-electron relaxation time τ satisfy the relation $\omega\tau \gg 1$, and the Drude term in the simplest model of a single frequency independent τ decreases monotonically with ω:

$$\epsilon_{2D} \propto \omega_p^2/\omega^3\tau ,$$

where ω_p is the conduction-electron plasma frequency. To make the separation we have assumed a more general form $\epsilon_{2D} = A\omega^{-B}$ and have found the constants A and B from the experimental variation of ϵ_2 below the first absorption edge where $\epsilon_{2\,ib}$ is zero. The values found for B were nearer in value to 2 than to the 3 of the simple Drude theory, a fact which has been noted by other authors but is

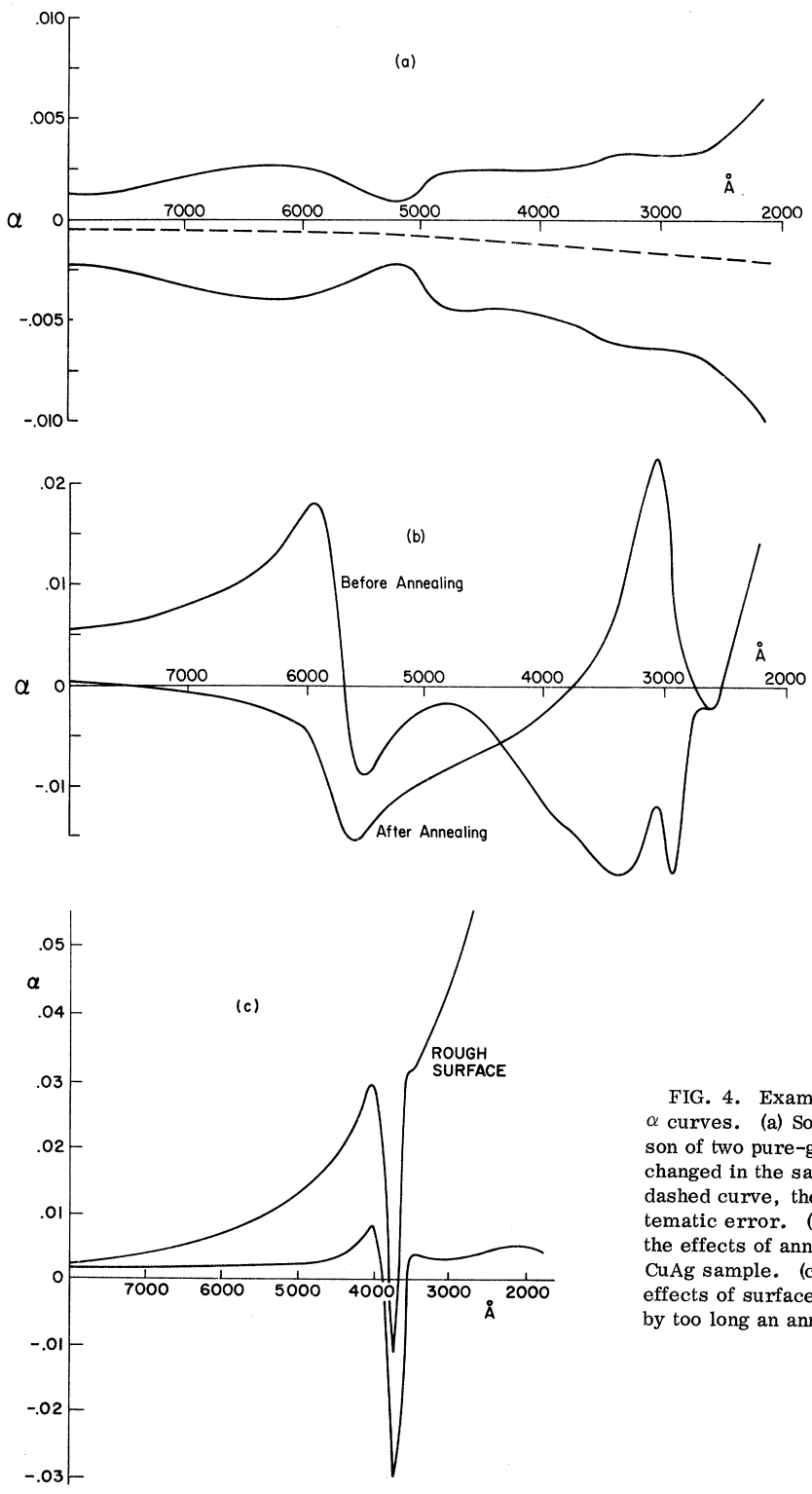

FIG. 4. Examples of experimental α curves. (a) Solid curves, comparison of two pure-gold samples interchanged in the sample-holding disk; dashed curve, the instrumental systematic error. (b) Illustration of the effects of annealing, 0.6-at.% CuAg sample. (c) Illustration of the effects of surface roughness produced by too long an anneal, AgAu sample.

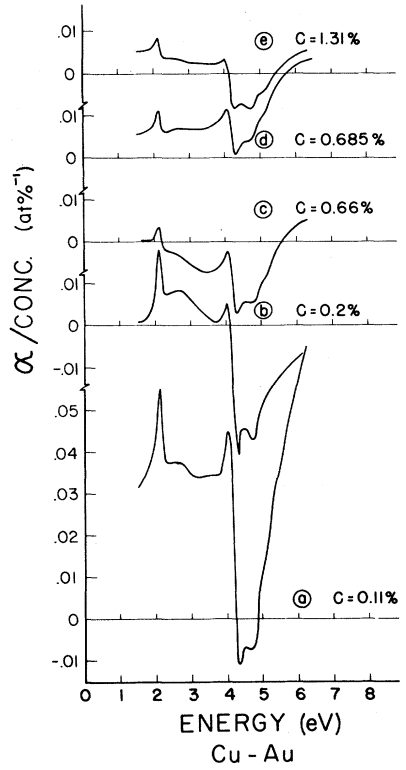

FIG. 5. Experimental curves of α/c vs photon energy for the CuAu system. The various curves are for differing alloy concentration c (at.%).

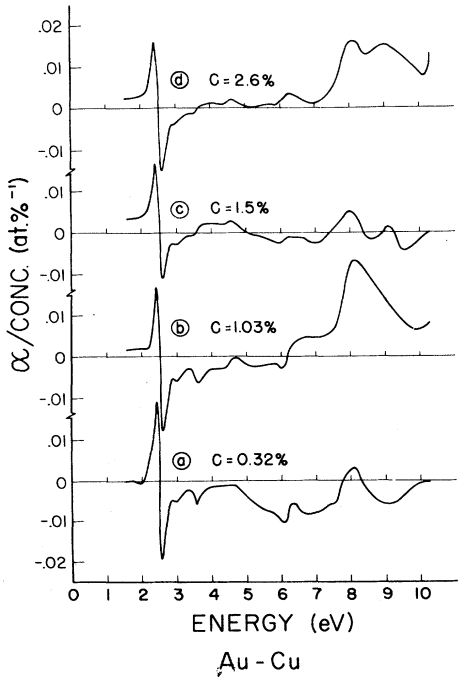

FIG. 6. Experimental curves of α/c vs photon energy for the AuCu system. The various curves are for differing alloy concentration c (at.%).

not yet satisfactorily explained. In Fig. 11 we show $\epsilon_{2\,\mathrm{ib}}$ spectra for the pure metals, as well as its energy derivative $d\epsilon_{2\,\mathrm{ib}}/dE$ (with E in eV). The peaks in the derivatives occur at interband thresholds. The identification of these thresholds by piezoreflectance measurements led to the band-gap assignments which were tabulated in Table I.

VI. ALLOY-INDUCED CHANGES IN DIELECTRIC CONSTANT

We turn to the alloy data. The difference property of the measurement was carried through in this analysis. We have first estimated the ratio of alloy to pure reflectivities from the experimental data α, $R_a/R_p = (1-\alpha)/(1+\alpha)$. We have then calculated ϵ_{1p} and ϵ_{2p} for the pure metal using R_p

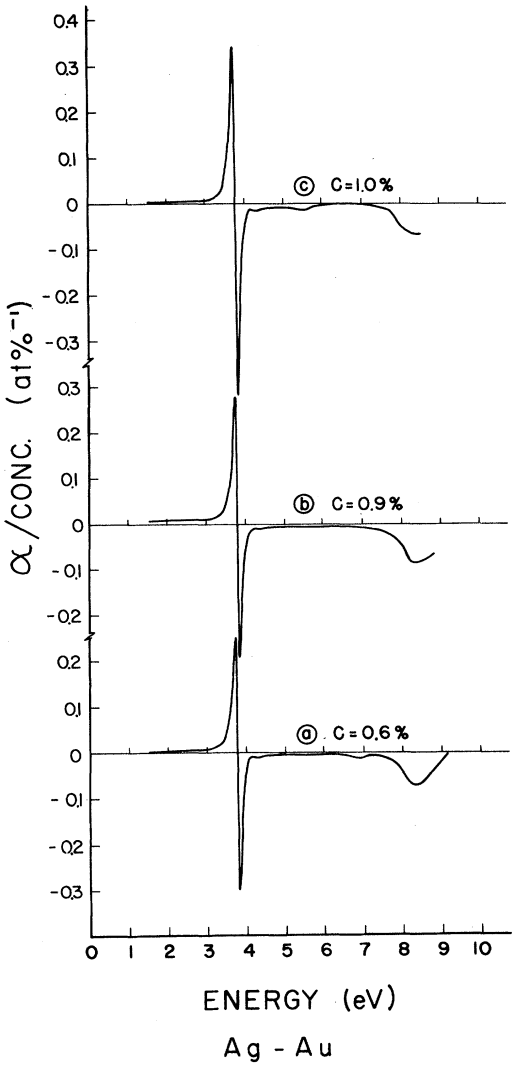

FIG. 7. Experimental curves of α/c vs photon energy for the AgAu system. The various curves are for differing alloy concentration c (at.%).

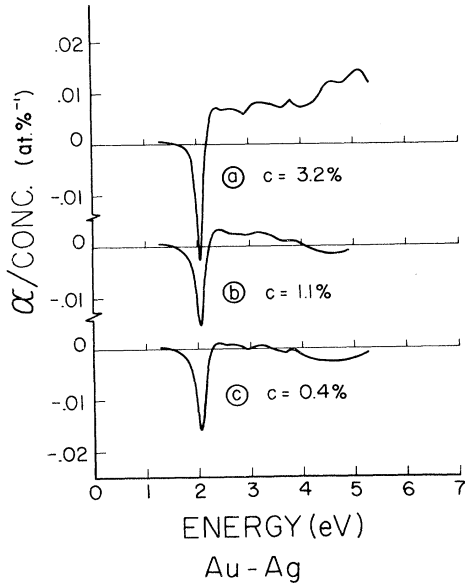

FIG. 8. Experimental curves of α/c vs photon energy for the AuAg system. The various curves are for differing alloy concentration c (at.%).

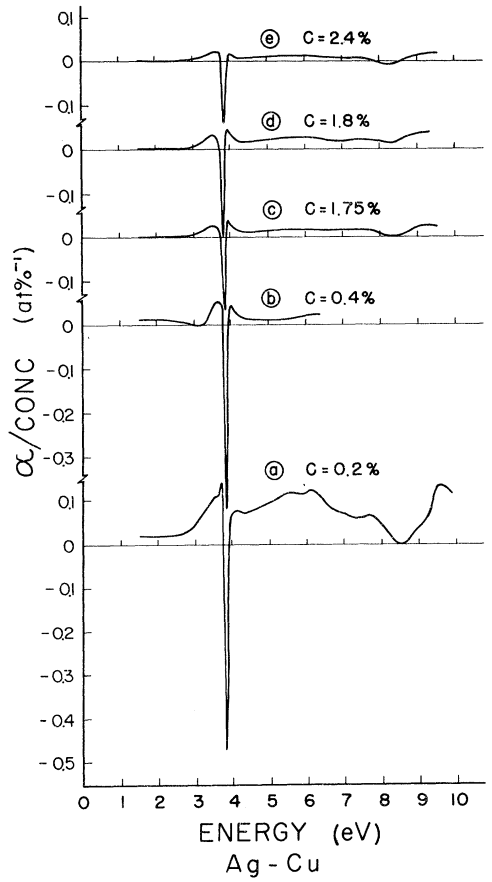

FIG. 9. Experimental curves of α/c vs photon energy for the AgCu system. The various curves are for differing alloy concentration c (at.%).

TABLE I. Energies and identification of the dominant transitions in the noble metals.

Copper		Silver		Gold	
eV	Identification[a]	eV	Identification	eV	Identification[b]
2.1	d–FS	3.9	d–FS	2.5	d–FS, significant X component
3.9	X_5–X_4'	4.15	L_2'–L_1[c]	2.9	
4.1	E_F–L_1	5.5	?	3.55	L_6^-–L_6^+
4.3	L_2'–L_1			4.5	X_7^+–X_6^+ ?
4.8	L_1^1–FS				

[a]Reference 23.

[b]Reference 24.

[c]Reference 25. No single-crystal piezostudies have been carried out on silver, and identifications are consequently less certain.

as data, and then repeated the calculation with $R_p[(1-\alpha)/(1+\alpha)] = R_a$ as data, to give ϵ_{1a} and ϵ_{2a}. The difference between the pure and alloy values has provided the changes due to alloying:

$$\Delta\epsilon_1 = \epsilon_{1p} - \epsilon_{1a}, \quad \Delta\epsilon_2 = \epsilon_{2p} - \epsilon_{2a}.$$

The data were normalized to changes per unit atomic-percent impurity by dividing by the concentration. The Kramers-Kronig procedure required assumptions about the behavior of α at low and high energies, beyond the region of measurement. With these dilute noble alloys the change in τ was less than a factor of 2 and the point where $\omega\tau$ equalled unity still lay in the infrared. The Drude model suggests that α should be constant in the region $\omega\tau \gg 1$, and we have made this assumption below

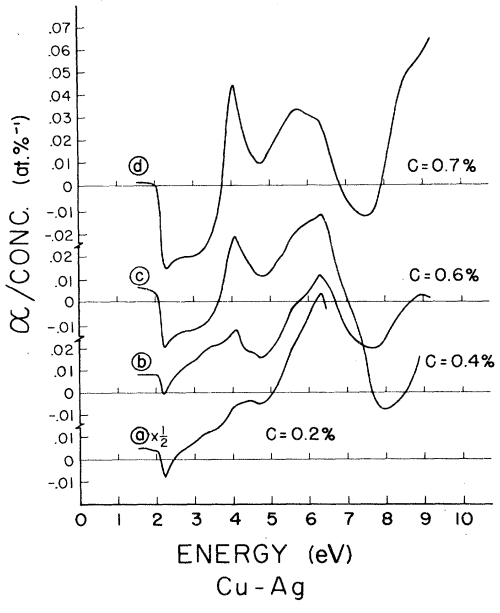

FIG. 10. Experimental curves of α/c vs photon energy for the CuAg system. The various curves are for differing alloy concentration c (at.%).

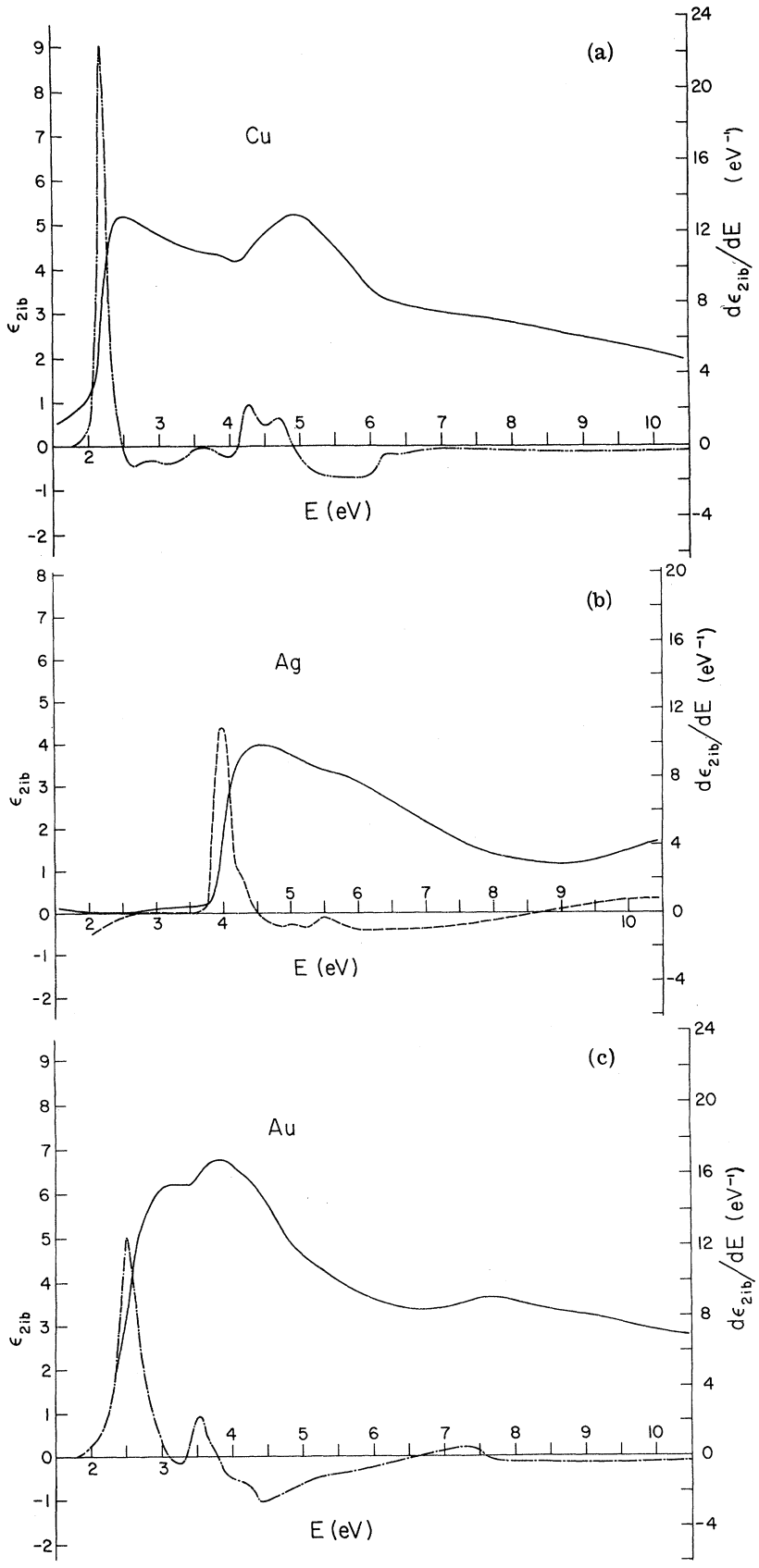

FIG. 11. $\epsilon_{2\,1b}$ (solid curve) and $d\epsilon_{2\,1b}/dE$ (dot-dash curve, E in eV) for (a) copper, (b) silver, (c) gold.

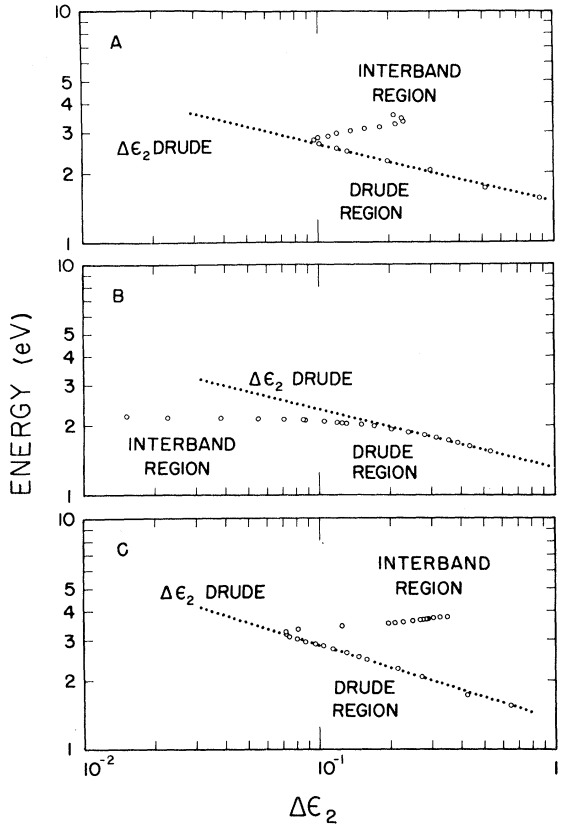

FIG. 12. Illustration of the $\Delta\epsilon_2$ curves, plotted as $\ln\Delta\epsilon_2$ vs $\ln E$, and of the separation into Drude and interband contributions. Example A is a AuCu sample, example B a CuAg sample, and example C a AgAu sample. The separation into Drude and interband regions is clear.

1.5 eV. Beyond 9 eV in the ultraviolet we have extrapolated α to zero smoothly on an energy scale.

$\Delta\epsilon_2$ is again a sum of two contributions, changes in the conduction-electron Drude term and changes in the interband term:

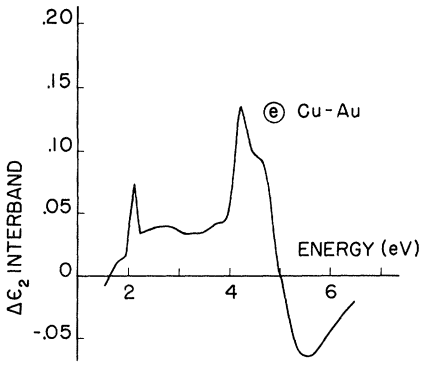

FIG. 13. $\Delta\epsilon_{2\,ib}/c$ vs E for CuAu; analysis of curve (e) of Fig. 5, concentration 1.3 at.%.

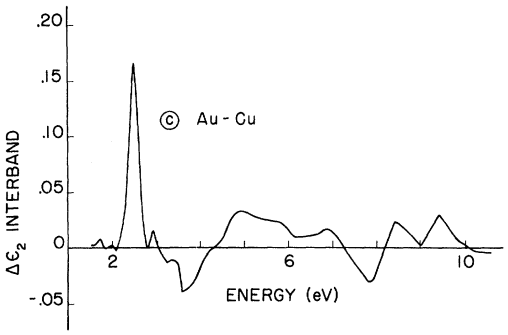

FIG. 14. $\Delta\epsilon_{2\,ib}/c$ vs E for AuCu; analysis of curve (c) of Fig. 6, concentration 1.5 at.%. Note that $\Delta\epsilon_{2\,ib}$ at the lowest-energy interband edge is positive as it is in Fig. 13, indicating edge shifts for both to lower energy.

$$\Delta\epsilon_2 = \Delta\epsilon_{2D} + \Delta\epsilon_{2\,ib}\,.$$

Since both the intraband terms for the alloy and the pure metal should be smoothly decreasing functions of frequency ($\omega\tau \gg 1$), we have carried out the separation in the same manner as for ϵ_{2p}. In Fig. 12 we show typical curves for $\Delta\epsilon_2$ plotted as $\ln\Delta\epsilon_2$ vs $\ln E$ illustrating the Drude and interband regions, with the Drude term shown as the dotted line. In Figs. 13–18 we show $\Delta\epsilon_{2\,ib}/c$ for the six alloy series. The samples analyzed have been chosen from the linear region of reflectance changes, and the small letters *a*, *b*, ... refer to the particular α curves which have been analyzed (see Figs. 5–10).

VII. INTERPRETATION OF DIELECTRIC-CONSTANT DATA

A. Interband Behavior

Before turning to the data, it is worth considering the type of behavior one might expect to observe. The sharp features in the $\epsilon_{2\,ib}$ spectra result from critical points in the interband density of states occurring at certain band gaps. If the band gap is

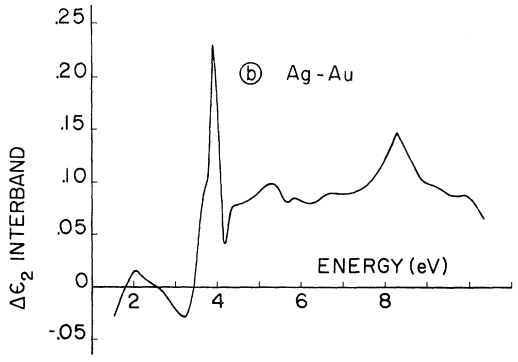

FIG. 15. $\Delta\epsilon_{2\,ib}/c$ vs E for AgAu; analysis of curve (b) of Fig. 7, concentration 0.9 at.%.

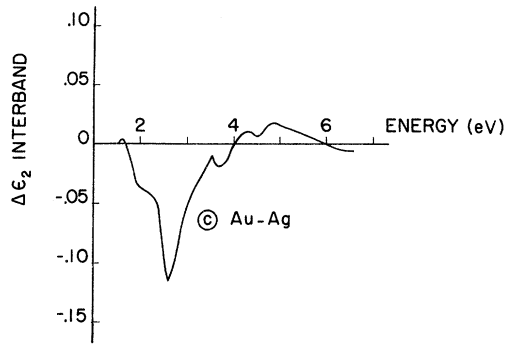

FIG. 16. $\Delta\epsilon_{2\,ib}/c$ vs E for AuAg; analysis of curve (c) of Fig. 8, concentration 0.4 at.%. $\Delta\epsilon_{2\,ib}$ at the lowest-energy interband edge is negative, of the opposite sign to Fig. 15, indicating edge shifts in opposite directions.

shifted in energy by an amount ΔE as a result of alloying, then the resulting $\Delta\epsilon_{2\,ib}$ would be just $\Delta\epsilon_{2\,ib} = -(d\epsilon_{2\,ib}/dE)\Delta E$. The peak in $\Delta\epsilon_{2\,ib}$ would lie at the point of maximum slope—see Fig. 19(a). If the band gap broadened owing to, for instance, lifetime effects, then one would observe a resonancelike $\Delta\epsilon_{2\,ib}$ with zero value at the point of maximum slope; see Fig. 19(b). Finally, if the host and impurity electrons each maintained their individual character with the same energy structure as in the pure materials, one would expect to see just a concentration effect (since ϵ_2 is proportional to the power absorbed per unit volume); $\Delta\epsilon_{2\,ib} = -c\epsilon_{2\,ib}(h) + c\epsilon_{2\,ib}(i)$ [see Fig. 19(c)]. Actually, the impurity states in this case would probably be quite different from those of the pure metal, and the positive part of $\Delta\epsilon_{2\,ib}$ will rather give an indication of the impurity energy distribution in this host. We shall use these three types of behavior to analyze the experimental data.

a. CuAu, Fig. 13. We see two main peaks which occur at the same energies as the derivative peaks—the two main gaps are thus shifting in energy on alloying. The second (higher-energy) peak is considerably larger than the first, the reverse of the derivative peaks, indicating that the conduction-electron $L_2' L_1$ gap is shifting a good deal more than the d–Fermi-surface gap; this was also found in the piezoreflectance measurements,[23,24,26] and the $\Delta\epsilon_{2\,ib}$ here is very similar to that resulting from from a volume expansion of pure copper; see Fig. 2 of Ref. 23(a).

b. AuCu, Fig. 14. Peaks are observed at 2.5, 3.5, and 4.5 eV, as in the derivative curves, indicating shifting gaps. A secondary peak at 2.9 eV is also observed, which is not resolved in the derivative curve.

c. AgAu, Fig. 15. A main peak at 3.9 eV and subsidiary peaks at 4.3 and 5.5 eV are observed, as in the derivative curve, indicating shifting gaps.

d. AuAg, Fig. 16. Negative peaks at 2.5 and 4.5 eV (the latter superimposed upon a positive background) and a positive peak at 3.5 eV are observed, the peaks being at the same energy as those in the derivative curve. The secondary peak at 2.9 eV which was resolved in the AuCu data occurs here only as a shoulder. The shoulder at 2.1 eV also suggests some broadening in these data.

e. AgCu, Fig. 17. The data for this alloy are completely different from that of AgAu above. Rather than a peak at 3.9 eV, we find a large positive contribution below the edge and a large negative contribution above the edge, the latter being similar in shape to the $\epsilon_{2\,ib}$ curve for silver. This we interpret as additive behavior for the electron states. The main edge does not shift, but, rather, the strength of the absorption is decreased, with a contribution below the edge from the copper-impurity states. The small sharp dip at 4.1 eV indicates shifting of this gap, however, which is associated with conduction-electron excitation rather than with d excitations.

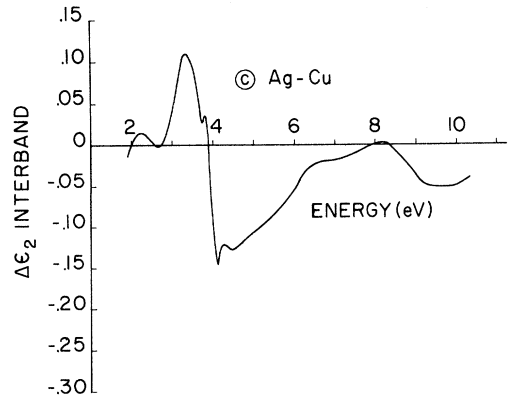

FIG. 17. $\Delta\epsilon_{2\,ib}/c$ vs E for AgCu; analysis of curve (c) of Fig. 9, concentration 1.75 at.%.

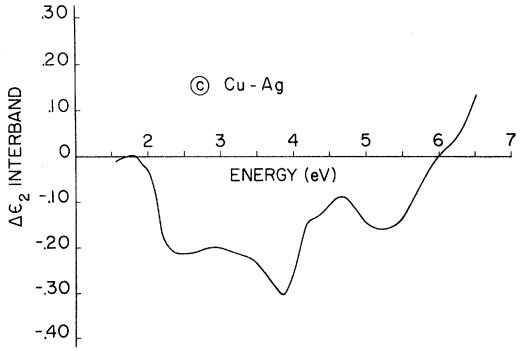

FIG. 18. $\Delta\epsilon_{2\,ib}/c$ vs E for CuAg; analysis of curve (c) of Fig. 10, concentration 0.6 at.%. Note that Figs. 17 and 18 have little resemblance to the derivative curves of Fig. 11.

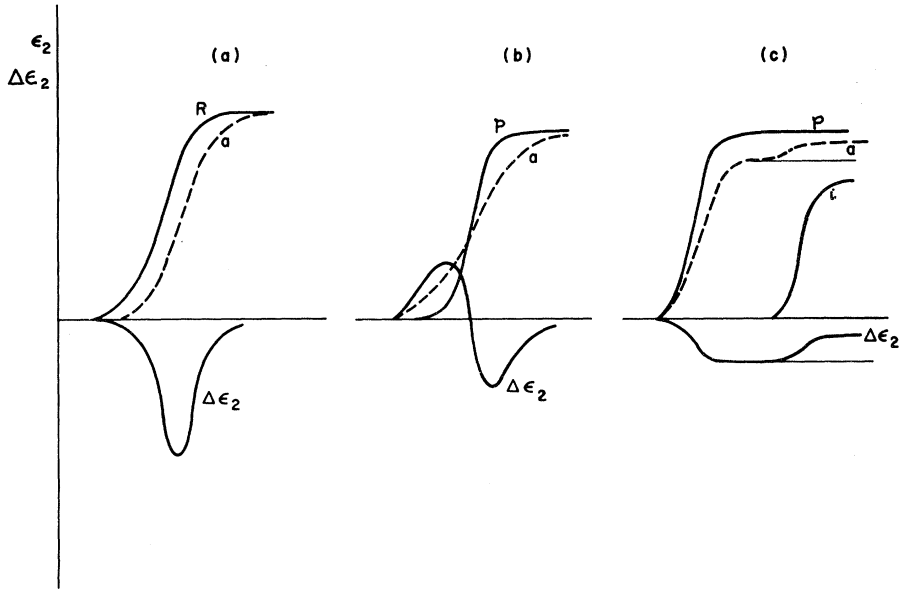

FIG. 19. $\Delta\epsilon_{2\,ib}$ behavior resulting from (a) a shift in the interband edge, (b) a broadening of the interband edge, and (c) additive $\epsilon_{2\,ib}$. p, a, i refer to the pure, alloy, and impurity spectra, respectively.

f. CuAg, Fig. 18. Between 2 and 4 eV there occurs a large negative contribution indicating an over-all decrease in the strength of the copper absorption. Between 4 and 5 eV, and 6 and 8 eV, there appear positive contributions superimposed upon the copper decrease. The interpretation of this is difficult, since the copper conduction-electron gap and the silver interband region commence at about the same energy. The peak and hump between 4 and 5 eV, however, are similar to those of CuAu, so we suggest that the region between 4 and 5 eV is associated with shifts of the copper conduction-electron gap, while the 6–8-eV region is due to excitation of the silver-impurity d states.

Table II summarizes the data for all these alloys. For the first four we list the shifts in gap energies per atomic percent of impurity derived, from the derivative data and the expression

$$\frac{\Delta E}{c} = -\frac{\Delta\epsilon_{2\,ib}}{c} \Big/ \frac{d\epsilon_{2\,ib}}{dE} \quad .$$

For the copper-silver alloys we list the fractional decrease in the host d absorption per atomic percent, $(\Delta\epsilon_{2\,ib}c^{-1})/\epsilon_{2\,ib}(p)$, and the energies at which the impurity d absorption occurs. For these latter we also list shifts of the conduction-electron gaps, but in view of the difficulty of separating these from the general host d decrease, the values are only very approximate. The values in this table have been taken from Figs. 13–18, and these in turn come from just one of the experimental curves for each alloy. In brackets we indicate the range of variation for the experimental α/c structure for alloys of different concentrations in the linear region. Some of this variation comes from uncertainty in the alloy concentration, and some from the nonlinear behavior which we observe at low concentrations. The values in brackets should thus be taken as measuring the absolute errors in these energy shifts and ϵ_2 changes. The relative errors between shifts of different parts of the spectrum are a good deal smaller since the relative magnitudes of the experimental structure tend to be independent of concentrations. (This is not so true of the copper-silver alloys.)

The values for the silver-gold alloys are within experimental error of those of Rivory.[10]

B. Effects of Changes in Lattice Constant

We have commented that the $\Delta\epsilon_{2\,ib}$ measurement for CuAu alloys resembles remarkably the $\Delta\epsilon_2$ resulting from a volume expansion of the pure-copper lattice. This indicates the necessity for taking into account the energy shifts associated with lattice changes. Fortunately, piezoreflectance measurements are now available on single crystals of copper[23] and gold,[24] where the volume can be separated from shear effects. Also, polycrystalline films of copper, silver, and gold have been compared[26] which provide an estimate for the changes for silver. Pearson[5] summarizes the lattice constants of the six dilute alloys—in Table III we list the relative volume changes per atomic percent for these alloys, and also the lattice constants of the pure metals.

Taking values directly from the experimental piezodata referred to above, we list in Table II the $\Delta\epsilon_2$ at the main gaps resulting from a 100% change in lattice constant $[\frac{1}{3}(W_{11}+2W_{12})$ in Gerhardt's notation[23]]. In this same table we have calculated the energy shift in these gaps corresponding to the change in lattice constant induced by 1 at. % of im-

TABLE II. Values for band-gap shifts, etc. on alloying.

		$\Delta\epsilon_2/c$ (at.%$^{-1}$)			$\Delta E/c$ (eV/at.%)	
Copper		Experiment	Lattice	Potential	Experiment	Potential
2.1 eV	CuAu	0.07 (± 5%)	0.095	−0.025	−0.0033	0.001
4.3 eV	CuAu	0.10 (± 25%)	0.124	−0.024	−0.04	0.01
	CuAg	0.08 (± 25%)	0.131	−0.05	−0.033	0.02
		Energy of silver impurity 7.5 eV; $\frac{\Delta\epsilon_2/c}{\epsilon_2(p)} = -0.026$				
Silver[a]						
3.9 eV	AgAu	0.28 (± 12%)	−0.005	0.285	−0.025	−0.026
4.1 eV	AgCu	−0.05 (± 15%)	−0.072	0.022	0.021	−0.009
	AgAu	0.03 (± 100%)	−0.005	0.035	−0.012	−0.014
		Energy of copper impurity 3.4 eV; $\frac{\Delta\epsilon_2/c}{\epsilon_2(p)} = 0.05$				
Gold						
2.5 eV	AuCu	0.23 (± 10%)	−0.022	0.252	−0.018	−0.019
	AuAg	−0.12 (± 5%)	0.0007	−0.121	0.009	0.009
3.5 eV	AuCu	0.06 (± 50%)	−0.10	0.16	−0.025	−0.067
	AuAg	0.015 (± 25%)	0.003	0.018	−0.006	−0.007
4.5 eV	AuCu	−0.06 (± 25%)	0.025	−0.085		
	AuAg	−0.015 (± 10%)	−0.001	−0.014		

The following values have been used to obtain these data.

Transition (eV)		$\frac{d\epsilon_2}{dE}$ (eV^{-1})	$W_{11}+2W_{12}$
Copper	2.1	21	62
	4.3	2.4	80
Silver[a]	3.9	11	60
	4.1	2.4	80
Gold	2.5	13	26
	3.5	2.4	118
	4.5	...	−30

[a]The 3.9- and 4.1-eV transitions in silver are not separately resolved in the piezoreflectance data. The total value for $W_{11}+2W_{12}$ is about 150. We have divided the two contributions in the same ratio as observed for copper. Similarly, we have used the copper and gold value for $d\epsilon_2/dE$ for the 4.1-eV transition.

purity. Finally, we list the difference between the experimental energy shift on alloying and that part estimated as being due to the changes in the lattice constant. This difference results from the differences in the host and impurity potential and we call it the "potential effect." Notice that the potential term is very small in the CuAu alloys, and much stronger in the AuCu alloys, while the lattice effect in the silver-gold alloys is negligible, the shifts in band gaps being entirely due to the potential effect.

C. Intraband Behavior

While our measurements in the infrared have not been sufficiently accurate to provide direct information on the changes in the intraband behavior,

TABLE III. Lattice constants of the pure metals and relative changes in volume per atomic percent on alloying.[a]

Host	a (kx)	$\frac{\Delta V}{V}/c \times 10^3$ (at.%$^{-1}$)
Copper	3.607	
-silver		4.9
-gold		4.6
Silver	4.078	
-copper		−2.7
-gold		−0.27
Gold	4.070	
-copper		−2.5
-silver		0.075

[a]Values taken from Pearson, Ref. 5.

TABLE IV. Relative changes in the conduction-electron effective mass per atomic-percent impurity.

	m^*		$\frac{\Delta m^*/m^*}{c}$ (at.%$^{-1}$)
Copper	1.45	CuAg	-0.004 ± 0.014
		CuAu	-0.002 ± 0.005
Silver	0.9	AgCu	0.013 ± 0.010
		AgAu	-0.011 ± 0.007
Gold	0.97	AuCu	-0.004 ± 0.002
		AuAg	-0.004 ± 0.003

using a generalization of our earlier procedure[27] we have been able to deduce a certain amount of information from a knowledge of the interband behavior. ϵ_1 is the sum of the intraband and interband terms,

$$\epsilon_1(\omega) = 1 - \frac{\omega_p^2}{\omega^2} + \epsilon_{1\,ib}(\omega) ,$$

where we use the Drude intraband expression for the limit $\omega\tau \gg 1$. The frequency-dependent interband term is related to $\epsilon_{2\,ib}$ by the Kramers-Kronig relation:

$$\epsilon_{1\,ib}(\omega_0) = \frac{2}{\pi} \int_0^\infty \frac{\omega \epsilon_{2\,ib}(\omega)\, d\omega}{\omega^2 - \omega_0^2} .$$

In the earlier paper we calculated $\epsilon_{1\,ib}$. Taking the difference between the experimental ϵ_1 curve and this $\epsilon_{1\,ib}$, we obtained values for ω_p^2 and so for the optical effective mass $m^* = 4\pi n e^2/\omega_p^2$. The generalization here is to take the difference between experimental $\Delta\epsilon_1$ and $\Delta\epsilon_{1\,ib}$ values, the latter calculated from the $\Delta\epsilon_{2\,ib}$, and thus to find relative changes in the optical effective mass $(\Delta m^*/m^*)c^{-1}$. We have

$$\Delta\epsilon_1(\omega_0) = \frac{\Delta\omega_p^2}{\omega_0^2} + \frac{2}{\pi} \int_0^\infty \frac{\omega \Delta\epsilon_{2\,ib}\, d\omega}{\omega^2 - \omega_0^2}$$

and

$$\Delta m^*/m^* = -\Delta\omega_p^2/\omega_p^2 .$$

The changes are small, but significant. The values are listed in Table IV, these being concentration-weighted averages of the results for all the samples of each dilute alloy and the errors being the concentration-weighted mean-square deviation from the average value. We list also the values for m^* for the pure metals. While the errors compared with the changes are not small, it is encouraging to see that in the case of the gold-silver alloys the changes are very close to those measured by Rivory.[10]

VIII. ELECTRONIC STRUCTURE OF ALLOYS

In this final section we will discuss those results which appear to us to be of particular interest.

A. Separate and Single Bands

Multiple-scattering theory has been used to formalize the full range of alloy behavior, giving the weak and strong limits, and showing the transition from one to the other. A theory called the coherent-potential approximation based on tight-binding electron states has been developed by Soven,[2] Onodera and Toyozawa,[3] and Velicky, Kirkpatrick, and Ehrenreich.[4] (Note that Stern[28] has recently questioned the use of localized electron states.) The important parameter in the theory is δ/w, where δ is the separation in energy between the states in the two metals and w is their bandwidth (taken to be the same). The theory predicts that when $\delta/w < 0.25$ the bands move smoothly from those of one metal to those of the other; when $\delta/w < 0.5$ the bands never coalesce but maintain their individual character, while when $0.25 < \delta/w < 0.5$ there is a range at low concentrations when the bands are separate, but at larger concentrations they join to form one band. The theory has been generalized to the case of different bandwidths on the two metals and the alloy by Berk[29] for small δ/w, and recently Levin and Ehrenreich[30] have included a hybridizing s band.

The difficulty in applying these ideas to real alloys lies in knowing what values to take for the energies and bandwidths. The first is the more difficult to determine. In our earlier brief report on these experiments[15] we assumed that the bottom of the conduction bands for each metal should be taken as a common energy level. Electrons with lower energy than this are bound to one atom, while electrons with higher energy move freely through the metal. We felt that this level acted in a very similar way to the vacuum level for electrons in an atom where the electrons are bound by their ionization energy. However, after further consideration we think this argument is probably too simple. In the tight-binding approach the energies are just the atomic-energy values. These would be appropriate for core states, but the energies of the noble-metal d electrons are sensitive to their conduction-electron environment. Watson, Ehrenreich, and Hodges[31] have suggested that through the renormalization of the outer s electron (because it must lie completely within one cell) the d energies are shifted by about 0.5 Ry from their free-atom values. This value for the shift was arrived at by calculation and by comparing certain band calculations with the free-atom values; it should be used rather tentatively since absolute energy values from other calculations vary con-

siderably. The physical process, however, seems sound. Indeed, Gerhardt[23(b)] has found experimentally that the d energy in copper depends upon the lattice constant, which indicates an environment effect, while Davis, Faulkner, and Joy[32] found the same effect in band calculations at different lattice constants.

There is an additional complication associated with the different lattice constants of the pure metals, since the energies and widths depend upon the lattice constant. Energies for the impurity states must be taken at the lattice constant of the host.

In Table V we have listed absolute energies of the bottom of the conduction band and the mean d energies and bandwidths from calculations found in the literature. Copper has been studied more thoroughly than the other noble metals, and the various calculated values are not so widely spread. For gold, relativistic calculations show rather lower energies than nonrelativistic calculations. The range of variation of these energies emphasizes the extreme difficulty in calculating absolute values. In the same table we show the energy of a d electron in the free atom, taken as $E_{da}=M^{II}-M^{I}$, where M^{I}, M^{II} are the one- and two-electron ionization energies, respectively. The shifts from the free atom to the metal are somewhat smaller than the "renormalization" shifts given by Watson, Ehrenreich, and Hodges (and Levin and Ehrenreich[30]).

The uncertainties in these absolute energies have made our attempts to estimate the model parameters at this stage meaningless—to our mind this remains one of the most challenging problems in alloy theory.

B. Aspects of Copper-Gold and Silver-Gold Single-Band Systems

1. d-Fermi-Surface Gap

Consider first the simpler silver-gold system. Stern,[33] analyzing the reflectance data of Wessel[8] and Rivory,[10] has shown that the d–Fermi-surface gap does not change linearly between silver and gold. We have found the same result. The rate of change of the gap was 0.009 eV/at.% at the gold-rich end, and 0.025 eV/at.% at the silver-rich end. Even at constant volume several effects cause this gap to change—changes in the mean d energy, changes in the d bandwidth, and changes in the Fermi level as a result of the modifications of the conduction-band density of states from the conduction-band–d-band hybridization. The system is thus complicated and nonlinearity should thus not be unexpected. Also, in silver this edge is due to transitions near L, while in gold it is due to transitions near X. Stern[33] suggests that the nonlinearity indicates a preferential charging effect on the lower d state. Nonlinearity is also likely in the coherent-potential theory (see Berk's generalization

TABLE V. Computed energy values (Ry); Refs. 7 and 30.

	Γ_1	E_d [a]	W [b]	E_F
Copper				
Burdick (Chodorow)	−1.04	−0.603	0.237	−0.384
Segall (ℓ dependent)	−0.836	−0.476	0.266	−0.19
Snow and Waber	−0.957	−0.721	0.167	−0.43
Davis, Faulkner, and Joy	−1.147	−0.660	0.241	−0.467
Watson, Hodges, and Ehrenriech	−0.83	−0.399		
Atomic		−0.924		
Deformation energies [c] Davis, Faulkner, and Joy	$\frac{\partial\Gamma_1}{\partial e}=0.62$	$\frac{\partial E_d}{de}=-0.43$	$\frac{\partial \ln W}{\partial e}=-1.5$	
Silver				
Segall (Hartree)	−0.86	−0.56	0.24	−0.31
Segall (Hartree-Fock)	−0.78	−0.69	0.19	−0.22
Ballinger and Marshall	−0.92	−0.764	0.24	−0.355
Watson, Hodges, and Ehrenreich	−0.74	−0.625		
Atomic		−1.025		
Gold				
Ballinger and Marshall	−0.63	−0.396	0.39	−0.01
Ramchandani (relativistic)	−1.22	−0.85	0.47	−0.505
Kupratakuln (relativistic)	−1.13	−0.78	0.38	−0.46
Levin and Ehrenreich	−0.613	−0.325		
Atomic		−0.831		

[a] $E_d=\frac{3}{5}\Gamma_{25}'+\frac{2}{5}\Gamma_{12}$. [b] $W=L_3-L_1$. [c] $e=\partial V/V$.

TABLE VI. Energy-gap shifts: see text. The volume correction is calculated from experimental deformation potentials (Table II) assuming a linear variation over the Cu-Ag, Au volume difference. This makes the Cu $L_2'L_1$ gap negative, which is unphysical and implies some breakdown of linearity.

	Host (eV) A	Impurity (eV) B	Volume-corrected impurity (eV) B^*	B^*-A (eV)	Potential eV/at.%	K
			d-FS gap			
CuAg	2.1	3.9	4.46	2.36		
CuAu	2.1	2.5	2.69	0.69	0.001	−0.85
AgCu	3.9	2.1	1.65	−1.75		
AgAu	3.9	2.5	2.5	−1.4	−0.026	0.85
AuCu	2.5	2.1	1.65	−0.85	−0.02	1.33
AuAg	2.5	3.9	3.9	1.4	0.009	−0.35
			$L_2'-L_1$ conduction-electron gap			
CuAg	4.3	4.1	7.6	3.3	0.01	−0.7
CuAu	4.3	3.5	8.3	4.0	0.02	−0.5
AgCu	4.1	4.3	−0.7	−4.8	−0.009	−0.81
AgAu	4.1	3.5	3.5	−0.6	−0.014	1.3
AuCu	3.5	4.3	−0.7	−4.2	−0.067	0.60
AuAg	3.5	4.1	4.1	0.6	−0.007	−2.16

to different bandwidths). The gold states lie higher than the silver, and so the top of the silver d band will be most strongly perturbed on mixing in silver.

The situation is even more complicated in the copper-gold system due to their differing lattice constants. The energy gap actually becomes smaller when gold is added to copper, moving away from the value in pure gold, but we have seen that this is a lattice-constant effect. We should compare the energy gaps and rates of shift at the same volume; we have done this using the experimental piezode-formation-potentials for this gap,[23,24,26] assuming that the gap is linear in volume for the 32% volume difference between copper and gold.

Table VI summarizes the data. Following Stern,[33] we write the gap (at constant volume) as

$$E - E_A = (E_B^* - E_A)\,[x + Kx(1-x)]\,,$$

with x the concentration of the B component (B^* indicates that the energies of the B metal have been corrected to values at A's volume). The values for K in this case are −0.85 and 1.33 at the copper-rich and gold-rich ends, respectively, which are comparable with the values 0.85 and −0.35 for the silver-rich and gold-rich alloys of the silver-gold system.

2. *Conduction-Electron Gap*

Here we look at excitation of the conduction electrons from the Fermi surface in the vicinity of L to the first excited band. The relevant data are listed in Table VI. We see that with the exception of AgAu, the potential effect moves the gap *away* from its value in the volume-uncorrected impurity. The situation changes completely when we compare band gaps for host and impurity at the same volume. The potential effect then shows movement *towards* the impurity value, with the exception only of AuAg. The shifts are far from linear—the values of K are quite large—whereas we would have expected the alloy perturbation to be weaker here than in the d-band case, since the conduction-electron bandwidth is much greater than the d-band bandwidth. We suggest that the nonlinearity in this case is another indication of the importance of d-band hybridization in determining the L_1 energy level.

3. *Effective-Mass Changes*

For all alloys except AgCu we found decreases in the conduction-electron effective mass; see Table IV. Our results for silver-gold are close to those of Rivory.[10] The physical process involved here appears quite subtle. The optical effective mass may be written as

$$(m^*)^{-1} = \left\langle \frac{1}{\hbar^2}\,\frac{d^2E}{dk^2} \right\rangle ,$$

the average taken over all occupied states, or as an integral over the Fermi surface,

$$(m^*)^{-1} = \left(\frac{1}{12\pi^3 N\hbar}\right)\int v_F\, dS_F\,.$$

In this latter form the subtlety is evident, since despite the similarity for all the noble metals of their Fermi-surface topology, m^* for copper is considerably larger than for silver or gold. To understand the changes in any detail, it appears necessary to study the changes in conduction-electron hybridization with the d band carefully, particularly for the alloys involving gold where spin-orbit effects are large. However, a general pat-

tern may be observed in the data. If the impurity d states lie lower than those of the host, the changes in mass are smaller. This is particularly clear for the silver-copper alloys, where the change on adding copper to silver is three times that of adding silver to copper; for the other alloys the differences are about a factor of 2.

The coherent-potential theory suggests that in general the effective mass should increase on alloying,[34] so the model analyzed must still be much too simple to be applicable to real metals.

4. *Nonlinear Changes at Low Concentrations*

In all of our alloy studies we have observed nonlinear behavior at concentrations below about 1 at.%. Our understanding of this behavior is the following: At very low concentrations the impurities should be completely isolated from each other, and any behavior in this region will be linear in concentration. As the concentration increases the impurities will be closer to each other, and, for instance, strain fields and charge distributions located around the impurities will start to interact, and nonlinear behavior will be present. At higher concentrations when the impurities are so close that these fields become uniform, one should again be in a linear region. The intermediate region of nonlinearity should occur around 1-at.% concentration, since screening lengths are typically 1–2 atomic-cell dimensions and at 1 at.% about two in every nine atoms in a line is an impurity atom. It would be of interest to study how the lattice constant of an alloy varied in the low- and intermediate-concentration regions; we understand[35] that a study of this sort has not been so far carried out. Certainly beyond several percent changes in lattice constant are linear in concentration.[36,37]

IX. SUMMARY

Our main observations are thus the following. In copper-gold and silver-gold alloys the d bands shift continuously with energy, and we have measured the rate of shift of the main band gaps. We have found that lattice-constant changes strongly influence the alloy band gaps. In copper-silver alloys the d bands are found to maintain their individual identity. For the six noble alloys we have found approximate values for the changes in conduction-electron optical effective mass.

These measurements highlight the need for further theoretical studies along the lines of Watson, Ehrenreich, and Hodges, which compare the energies of d states in different metals, to study the effects of mixing d states on the over-all band structure of the alloys.

†Work supported by ARPA, AFOSR, and NSF.

*Now at Victoria University of Wellington, Wellington, New Zealand.

‡This research was carried out while the author was on sabatical at the University of Maryland, College Park, Md. 20742.

[1]J. Friedel, Nuovo Cimento Suppl. 7, 287 (1958).

[2]P. Soven, Phys. Rev. 156, 809 (1967).

[3]Y. Onodera and Y. Toyozawa, J. Phys. Soc. Japan 24, 341 (1968).

[4]B. Velicky, S. Kirkpatrick, and H. Ehrenreich, Phys. Rev. 175, 747 (1968).

[5]W. B. Pearson, *Handbook of Lattice Spacings and Structures of Metals and Alloys* (Pergamon, London, 1958).

[6]M. Hansen and K. Anderko, *Constitution of Binary Alloys*, 2nd ed. (McGraw-Hill, New York, 1958).

[7]Copper: B. Segall, Phys. Rev. 125, 109 (1962); G. Burdick, *ibid.* 129, 138 (1963); E. C. Snow and J. T. Waber, *ibid.* 157, 570 (1967); H. L. Davis, J. S. Faulkner, and H. W. Joy, *ibid.* 167, 601 (1968).

Silver: B. Segall, G. E. Report No. 61-RL-(2785G), 1961 (unpublished); E. C. Snow, Phys. Rev. 172, 708 (1968); R. A. Ballinger and C. A. W. Marshall, J. Phys. C 2, 1822 (1969).

Gold: C. B. Sommers and H. Amar, Phys. Rev. 188, 1117 (1970); M. G. Ramchandani, J. Phys. C Suppl. 3, S1 (1970); S. Kuprataknin, *ibid.* Suppl. 3, S109 (1970); J. W. D. Connolly and K. H. Johnson, Progress Report Solid State and Molecular Theory Group, MIT, No. 72, 1970 (unpublished); R. A. Ballinger and C. A. W. Marshall, J. Phys. C 2, 8122 (1969).

[8]P. R. Wessel, Phys. Rev. 132, 1062 (1963).

[9]H. Fukutani and O. Sueoka, in *Optical Properties and Electronic Structure of Metals and Alloys*, edited by F. Abeles (North-Holland, Amsterdam, 1966).

[10]J. Rivory, Opt. Commun. 1, 53 (1969).

[11]A. J. McAllister, E. A. Stern, and J. C. McGroddy, Phys. Rev. 140, A2105 (1965).

[12]L. F. Chollet and I. M. Templeton, Phys. Rev. 170, 656 (1968); P. E. King-Smith, Phil. Mag. 12, 1123 (1965).

[13]D. Beaglehole, Appl. Opt. 7, 2218 (1968).

[14]D. Beaglehole and T. J. Hendrickson, Phys. Rev. Letters 22, 133 (1969).

[15]D. Beaglehole and E. Erlbach, Solid State Commun. 8, 255 (1970).

[16]E. Erlbach and D. Beaglehole, *Proceedings of the Third* IMR *Symposium, Electronic Density of States* (U.S. GPO, Washington, D. C., 1970) Natl. Bur. Std., Special Publication No. 323.

[17]D. Beaglehole, Proc. Phys. Soc. (London) 85, 1007 (1965).

[18]J. O. Linde, Ann. Physik 15, 239 (1932).

[19]R. B. Dingle, Proc. Roy. Soc. (London) A201, 545 (1950).

[20]D. Beaglehole and O. Hunderi, Phys. Rev. B 2, 309 (1970).

[21]H. E. Bennett, M. Silver, and E. J. Ashley, J. Opt. Soc. Am. 53, 1089 (1963).

[22]H. Ehrenreich and H. R. Philipp, Phys. Rev. 128, 1622 (1962).

[23](a) U. Gerhardt, D. Beaglehole, and R. Sandrock, Phys. Rev. Letters 19, 309 (1967); (b) U. Gerhardt, Phys. Rev. 172, 651 (1968).